Z. angew. Math. Phys. 53 (2002) 281–307
0010-2571/02/020281-27 $ 1.50+0.20/0

Zeitschrift für angewandte Mathematik und Physik ZAMP

Exterior Stokes flows with stick-slip boundary conditions

D. Palaniappan and Prabir Daripa *

Abstract. Steady two-dimensional creeping flows induced by line singularities in the presence of an infinitely long circular cylinder with stick-slip boundary conditions are examined. The singularities considered here include a rotlet, a potential source and a stokeslet located outside a cylinder and lying in a plane containing the cylinder axis. The general exterior boundary value problem is formulated and solved in terms of a stream function by making use of the Fourier expansion method. The solutions for various singularity driven flows in the presence of a cylinder are derived from the general results. The stream function representation of the solutions involves a definite integral whose evaluation depends on a non-dimensional slip parameter λ_1. For extremal values, $\lambda_1 = 0$ and $\lambda_1 = 1$, of the slip parameter our results reduce to solutions of boundary value problems with stick (no-slip) and perfect slip conditions, respectively.

The slip parameter influences the flow patterns significantly. The plots of streamlines in each case show interesting flow patterns. In particular, in the case of a single rotlet/stokeslet (with axis along y-direction) flows, eddies are observed for various values of λ_1. The flow fields for a pair of singularities located on either side of the cylinder are also presented. In these flows, eddies of different sizes and shapes exist for various values of λ_1 and the singularity locations. Plots of the fluid velocity on the surface show locations of the stagnation points on the surface of the cylinder and their dependencies on λ_1 and singularity locations.

Keywords. Stokes flows, source, rotlet, Stokeslet.

1. Introduction

The study of low Reynolds number flows (Stokes flows) past obstacles has been the subject of theoretical and practical importance for well over a century and half. In his classic paper [1] (see also [2]), Stokes discussed solutions of creeping flow equations in the presence of two and three-dimensional objects. Since then there has been many applications of Stokes flows in the diverse fields of engineering, science and technology. Some perspectives on analytical and numerical methods for solving Stokes flow problems are documented in the standard reference books on the subject [3, 4, 5, 6]. In these monographs, major attention has been given to the solutions of creeping flow problems involving regular geometries such as spheres, spheroids, ellipsoids etc., and their degenerating cases.

* Author for correspondence

The corresponding two-dimensional Stokes flow problems have also received attention but less comparatively. The ill-posedness of some two-dimensional problems could be a possible cause for this. Indeed, Stokes [1] himself noticed that there is no solution for the uniform flow past a circular cylinder. This has come to be known as the 'Stokes paradox' and is true for any arbitrary two-dimensional obstacle. The full resolution of the paradox required the perspective of singular perturbation theory developed by Kaplun and Lagerstrom [7] and Proudman and Pearson [8]. These authors showed that Stokes equations, although valid near a boundary, are not uniformly valid throughout the domain of the flow. They further demonstrated the necessity of Oseen's approximation and confirmed the solution due to Oseen [9].

In some circumstances, two-dimensional stokes flow problems become well-posed and solutions have been found for some such flows. Jeffery [10] studied the slow viscous flow generated by two circular cylinders rotating with equal and opposite angular velocities. He discovered that such flows produce finite velocities far away from the cylinders. In particular, he showed that a uniform flow is generated at large distances from the rotating cylinders. This phenomenon is widely known as the 'Jeffery paradox'. The simplest example that illustrates this phenomenon was provided by Dorrepaal et al. [11] who noticed an uniform flow in the case of rotlet/stokeslet induced flows in the presence of a rigid cylinder. Subsequent works [12, 13] demonstrated the same phenomenon with singularities such as source, potential-dipole etc. Almost all these studies used the no-slip boundary conditions on the surface of the cylinder. However, there are situations where the fluid may slip on a boundary surface such as in rarefied gas dynamics [14]. The presence of slip can influence the flow as well as the physical quantities of interest which are addressed in this paper.

It should be pointed out that Stokes flow problems in three dimensions with stick-slip boundary conditions have been addressed in the literature. For instance, Basset [15] (see also [3]) solved the Stokes flow past a solid sphere with slip on the surface. Felderhof and coworkers [16, 17, 18, 19] developed schemes for arbitrary flow around spherical particles with stick-slip conditions. In their analyses, a new approach, borrowed from electromagnetic and scattering literature, was introduced. It was also found that the slip parameter influences the flow fields, drag and torque significantly. Recent articles [20, 21] further highlighted the role of slip parameter in Stokesian dynamics. Surprisingly, the effect of slip in two-dimensional Stokes flows has not been explored in detail to-date to the best of our knowledge. In this article, we investigate the role of slip on some singularity induced creeping flows in the presence of a cylinder.

The paper is organized as follows. In section **2**, the basic equations are given and using the Stokes stream function the problem is reformulated. The boundary conditions are then derived in terms of stream function and a brief discussion on the slip and no-slip constraints is provided. In section **3**, the general solution is derived by the use of Fourier expansion method. The solutions to various singularity driven

flow problems are presented in section **4**. The basic singularities considered here include rotlet, source and stokeslet. The effect of slip on the flow fields is discussed in each case. The flow description is illustrated in different situations through streamline plots. The plots of fluid velocity on the surface are also provided. The effect of slip parameter and primary singularity locations on the fluid velocity on the surface is discussed briefly in each case. The concluding remarks of the present analysis are presented in section **5**.

2. Mathematical formulation

We consider a two-dimensional steady creeping flow (Stokes flow) of a viscous incompressible fluid past an impenetrable infinitely long circular cylinder of radius a. The governing equations of motion are the linearized Navier-Stokes equations or simply Stokes equations given by

$$\nabla^2 q_r - \frac{q_r}{r^2} - \frac{2}{r^2}\frac{\partial q_\theta}{\partial \theta} = \frac{1}{\mu}\frac{\partial p}{\partial r}, \tag{2.1}$$

$$\nabla^2 q_\theta - \frac{q_\theta}{r^2} + \frac{2}{r^2}\frac{\partial q_r}{\partial \theta} = \frac{1}{\mu}\frac{1}{r}\frac{\partial p}{\partial \theta}, \tag{2.2}$$

$$\frac{\partial q_r}{\partial r} + \frac{q_r}{r} + \frac{1}{r}\frac{\partial q_\theta}{\partial \theta} = 0. \tag{2.3}$$

Here q_r and q_θ are the radial and tangential velocity components respectively, (r, θ) are the polar coordinates, μ is the coefficient of viscosity, p is the pressure and ∇^2 is the two-dimensional Laplacian operator,

$$\nabla^2 \equiv \frac{\partial^2}{\partial r^2} + \frac{1}{r}\frac{\partial}{\partial r} + \frac{1}{r^2}\frac{\partial^2}{\partial \theta^2}.$$

For two-dimensional flows, one can define

$$q_r = -\frac{1}{r}\frac{\partial \psi}{\partial \theta}, \quad q_\theta = \frac{\partial \psi}{\partial r}, \tag{2.4}$$

satisfying (2.3), where $\psi(r, \theta)$ is the stream function. Substitution of (2.4) in (2.1) and (2.2) yields

$$\nabla^4 \psi = 0. \tag{2.5}$$

Thus, the problem of steady two-dimensional Stokes flow reduces to solving scalar biharmonic equation (2.5) for ψ subject to appropriate boundary conditions on the cylinder. The no-slip or stick boundary conditions are often used in fluid dynamics. Here, we employ the stick-slip conditions on the boundary of the cylinder. In this case, the boundary conditions may be stated as follows.

- Normal velocity is zero on the boundary i.e., $q_r = 0$ on $r = a$.
- Fluid velocity is proportional to the tangential stress on the surface of the

cylinder i.e., $q_\theta = \frac{\lambda}{\mu} T_{r\theta}$, where

$$T_{r\theta} = \mu \left[\frac{1}{r} \frac{\partial q_r}{\partial \theta} + r \frac{\partial}{\partial r} \frac{q_\theta}{r} \right],$$

is the tangential stress and $\lambda \geq 0$ is the slip-length. In terms of stream function, these conditions become

$$\left.\begin{array}{l} \psi = 0, \\ \dfrac{\partial \psi}{\partial r} = \lambda r \dfrac{\partial}{\partial r} \dfrac{1}{r} \dfrac{\partial \psi}{\partial r} \end{array}\right\} \quad \text{on} \quad r = a. \tag{2.6}$$

Similar conditions were employed by Basset [15] to solve for the flow past a sphere in three dimensions. Felderhof and coworkers [16, 17, 19, 18] used the stick-slip conditions to discuss the scattering coefficients due to spherical particles suspended in any given unbounded flow field. Here we exploit these conditions to solve the singularity driven flow problems in the presence of a circular cylinder. It may be noticed that when $\lambda \to 0$, (2.6) reduces to the usual no-slip conditions and when $\lambda \to \infty$, it reduces to the perfect slip conditions.

In the present paper, we investigate the flows induced by the singularities of Stokes flow in the presence of a circular cylinder. In this case, in addition to (2.6) we have

$$\psi \sim \psi_0 \quad \text{as} \quad R_1 \to 0, \tag{2.7}$$

where ψ_0 corresponds to the basic flow in the absence of the cylinder and R_1 (see Fig. 1) is the distance of the field point measured from the singularity. In other words, flow in the immediate vicinity of the singularity is that of the basic flow. Below, we present the solution of the problem discussed above.

3. Method of solution

There are classical and numerical methods to solve (2.5) subject to the boundary conditions (2.6) and (2.7). The most suitable and commonly used technique is the Fourier expansion method. In this method, the given flow is expanded in a Fourier series with known Fourier coefficients. Then, the unknown coefficients of the perturbed flow (also written in a Fourier series) are computed with the aid of the boundary conditions. The other methods applicable to the present problem include the image method [11, 13] and the boundary integral equation method [22]. We adopt the Fourier representation technique for our problem and make an attempt to sum the resulting series solution. To this end, we write the given flow field in the absence of the cylinder as

$$\psi_0(r, \theta) = \sum_{n=0}^{\infty} [\alpha_n r^n + \beta_n r^{n+2}] f_n(\theta), \tag{3.1}$$

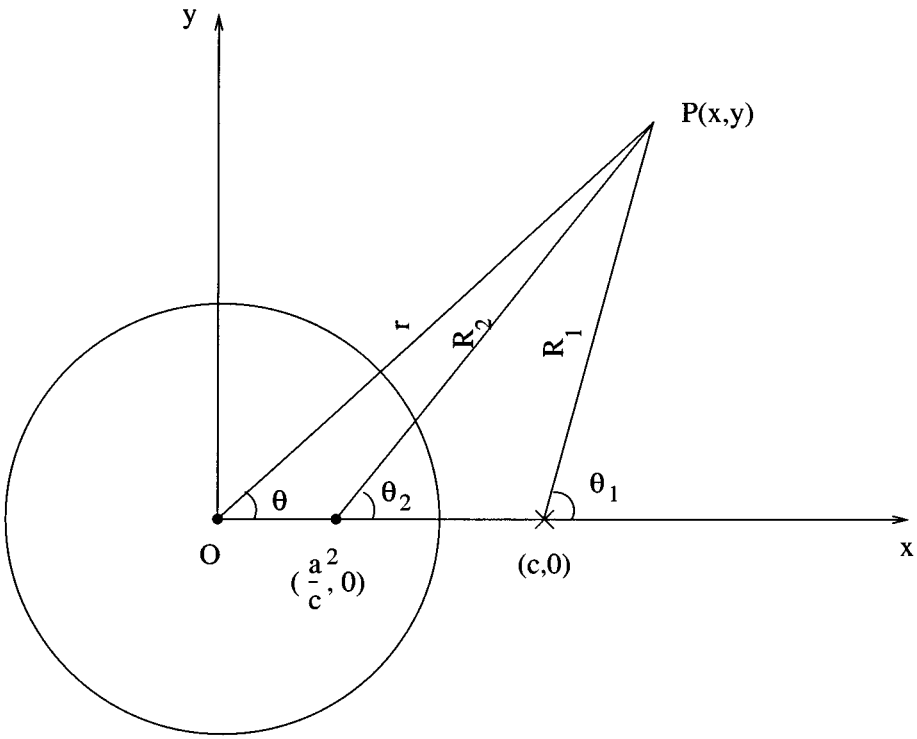

Figure 1. Definition of the coordinate system.

where $f_n(\theta) = \gamma_n \cos n\theta + \delta_n \sin n\theta$, and $\alpha_n, \beta_n, \gamma_n, \delta_n$ are known constants. The solution satisfying (2.5) in the presence of a circular cylinder can be taken as

$$\psi(r,\theta) = \psi_0 + \sum_{n=0}^{\infty} \left[\frac{A_n}{r^n} + \frac{B_n}{r^{n-2}} \right] f_n(\theta), \tag{3.2}$$

where A_n, B_n are unknown constants to be determined. We remark that the constants α_0 and β_0 corresponding to $n = 0$ may be adjusted in each problem by choosing appropriate A_0 and B_0. Applying the boundary conditions (2.6), we obtain

$$\frac{A_n}{a^n} = \left(-1 + \frac{n}{n\lambda_1 + 1 - \lambda_1} \right) \alpha_n a^n + \left(-1 + \frac{(n+1)(1-\lambda_1)}{n\lambda_1 + 1 - \lambda_1} \right) \beta_n a^{n+2}, \tag{3.3}$$

$$\frac{B_n}{a^{n-2}} = -\left(\frac{n}{n\lambda_1 + 1 - \lambda_1} \right) \alpha_n a^n - \left(\frac{(n+1)(1-\lambda_1)}{n\lambda_1 + 1 - \lambda_1} \right) \beta_n a^{n+2}, \tag{3.4}$$

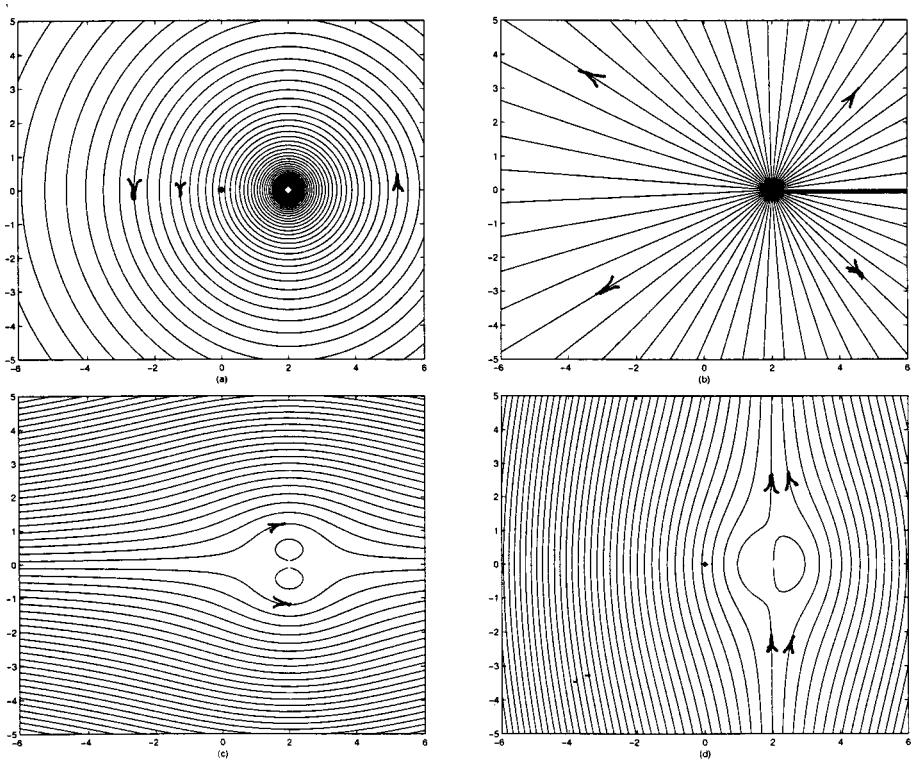

Figure 2. The streamline patterns of the four basic singularity driven flows without the cylinder. The singularity location is at $(x = 2.0, y = 0)$ in each case. (a) Rotlet; (b) Source; (c) Stokeslet along x-direction; (d) Stokeslet along y-direction.

where we have defined $\lambda_1 = \frac{2\lambda}{a+2\lambda}$, $0 \leq \lambda_1 \leq 1$. Following the terminology from the three-dimensional case [16, 17, 18], we refer the relations (3.3) and (3.4) above as scattering coefficients for a cylinder. The solution (3.2) with the scattering coefficients given by (3.3) and (3.4) is sufficient to discuss various two-dimensional problems. It is easy to see from (3.2)–(3.4) that $\psi = 0$ when $n = 1$ and $\beta_1 = 0$, implying that there is no solution for a uniform flow past a circular cylinder with stick-slip conditions. This, of course, is the well known 'Stokes paradox' originally demonstrated for a rigid circular cylinder by Stokes [1]. As said before, we derive solutions for singularity driven flows in the presence of a cylinder. We consider the basic flow due to (i) a rotlet (ii) a source (iii) a stokeslet (the streamline patterns for these basic flows in the absence of cylinder are shown in Fig. 2), and obtain the perturbed flow fields in each case in the presence of a cylinder. The solutions for higher order singularities in the presence of a cylinder may be derived in a similar manner. For the sake of completeness, we list below the velocity, the pressure and

the vorticity fields calculated from (3.2).

$$q_r = -\sum_{n=1}^{\infty}\left[\alpha_n r^{n-1} + \beta_n r^{n+1} + \frac{A_n}{r^{n+1}} + \frac{B_n}{r^{n-1}}\right] f_n'(\theta), \tag{3.5}$$

$$q_\theta = \sum_{n=1}^{\infty}\left[n\alpha_n r^{n-1} + (n+2)\beta_n r^{n+1} - n\frac{A_n}{r^{n+1}} - (n-2)\frac{B_n}{r^{n-1}}\right] f_n(\theta), \tag{3.6}$$

$$p = p_0 - 4\mu\sum_{n=1}^{\infty}\left[(n+1)r^n\beta_n + (n-1)\frac{B_n}{r^n}\right] f_n(\theta), \tag{3.7}$$

$$\omega = \sum_{n=1}^{\infty}\left[(2n+1)r^n\beta_n - (2n-1)\frac{B_n}{r^n}\right] f_n'(\theta). \tag{3.8}$$

Below, we present solutions for singularity induced Stokes flow problems in the presence of a circular cylinder.

4. Singularity driven flows past a cylinder

We now employ the solution scheme derived in the previous section (equations (3.2)-(3.4)) to various singularity driven flows in the presence of a cylinder. We show that the Fourier series solution can be summed to yield closed form expressions for the stream function in all cases. We then use the closed form analytic solutions to describe the flow fields and discuss their features. In particular, we demonstrate the effect of the slip parameter on the flow patterns and also on other physical quantities in each case.

4.1. A circular cylinder and a line rotlet

The stream function of the flow induced by a line rotlet of strength F located at $r = c > a$, $\theta = 0$ is given by

$$\psi_0 = F\log R_1,$$

where $R_1^2 = r^2 - 2cr\cos\theta + c^2$. The Fourier expansion of ψ_0 is given by

$$\psi_0 = F\log c - F\sum_{n=1}^{\infty}\frac{r^n}{nc^n}\cos n\theta. \tag{4.1.1}$$

In the present problem $\alpha_0 = F\log c$, $\beta_0 = 0$, $\gamma_n = 1$ and $\delta_n = 0$. Comparison of (3.1) and (4.1.1) for $n \geq 1$ yields

$$\alpha_n = -\frac{F}{nc^n}, \quad \beta_n = 0 \quad \text{for all} \quad n.$$

In the presence of a cylinder with its axis parallel to the axis of the rotlet, the scattering coefficients from (3.3) and (3.4) become

$$A_n = -F\left(-1 + \frac{n}{n\lambda_1 + 1 - \lambda_1}\right)\frac{a^{2n}}{nc^n}\alpha_n \tag{4.1.2}$$

$$B_n = F\left(\frac{1}{n\lambda_1 + 1 - \lambda_1}\right)\frac{a^{2n-2}}{c^n}\alpha_n. \tag{4.1.3}$$

We have chosen $A_0 = -F\log c, B_0 = 0$ corresponding to $n = 0$. Now, the stream function for the rotlet-cylinder combination becomes

$$\psi(r,\theta) = F\sum_{n=1}^{\infty}\left\{-\frac{r^n}{nc^n} - \left[-1 + \frac{n}{n\lambda_1 + 1 - \lambda_1}\right]\frac{a^{2n}}{nc^n r^n} + \left[\frac{1}{n\lambda_1 + 1 - \lambda_1}\right]\frac{a^{2n-2}}{c^n r^{n-2}}\right\}\cos n\theta. \tag{4.1.4}$$

The Fourier series expansion (4.1.4) can be summed to yield the following exact solution:

$$\psi(r,\theta) = F\left[\log R_1 - \log\frac{cR_2}{r} + \frac{1-\lambda_1}{\lambda_1}(a^2 - r^2)I_1\right], \tag{4.1.5}$$

where

$$I_1 = \frac{r^{\frac{1-\lambda_1}{\lambda_1}}}{a^{\frac{2}{\lambda_1}}}\int_0^{a^2/r}\rho^{\frac{1}{\lambda_1}-2}\left(-\log R_{1\rho} + \rho\frac{(\rho - c\cos\theta)}{R_{1\rho}^2}\right)d\rho, \tag{4.1.6}$$

$$R_2^2 = r^2 - \frac{2a^2}{c}r\cos\theta + \frac{a^4}{c^2}, \quad R_{1\rho}^2 = \rho^2 - 2c\rho\cos\theta + c^2. \tag{4.1.7}$$

The second and third terms in (4.1.5) are the image terms due to the presence of the cylinder. Interestingly the third term involves a definite integral (given in (4.1.6)) whose evaluation depends on the slip parameter λ_1. This in turn implies that the image system depends on the slip parameter. We note that for some values of λ_1, the integral can be evaluated analytically. For any value of λ_1 between 0 and 1, the integral may be computed numerically. The effect of slip on the image system may be demonstrated by evaluating the integral for specific values of λ_1. We note that if we set $\lambda_1 = 0$ in (4.1.5), we recover the results with no-slip boundary condition [11, 12]. The results for a pure slip boundary condition may be obtained by setting $\lambda_1 = 1$ in (4.1.5).

For a rotlet of strength F' located at (c', π), $c' > a$, the stream function in the absence of a cylinder is $\psi_0 = F'\log R_1'$, where ${R_1'}^2 = r^2 + 2c'r\cos\theta + {c'}^2$. The modified stream function in the presence of a cylinder may be constructed in the same way as explained above. The solution in this case is given by

$$\psi(r,\theta) = F\left[\log R_1' - \log\frac{cR_2'}{r} + \frac{1-\lambda_1}{\lambda_1}(a^2 - r^2)I_1'\right], \tag{4.1.8}$$

where

$$I_1' = \frac{r^{\frac{1-\lambda_1}{\lambda_1}}}{a^{\frac{2}{\lambda_1}}} \int_0^{a^2/r} \rho^{\frac{1}{\lambda_1}-2} \left(-\log R'_{1\rho} + \rho \frac{(\rho + c' \cos\theta)}{R'^2_{1\rho}} \right) d\rho, \tag{4.1.9}$$

$$R'^2_2 = r^2 + \frac{2a'^2}{c} r\cos\theta + \frac{a^4}{c'^2}, \quad R'^2_{1\rho} = \rho^2 + 2c'\rho\cos\theta + c'^2. \tag{4.1.10}$$

Next we discuss the the flow patterns due to rotlet(s) in the presence of a cylinder. The streamlines for a single rotlet are sketched using (4.1.5) while the streamlines for a pair of rotlets are plotted using (4.1.5) and (4.1.8). Various plots are shown for different values of the parameters λ_1, F, F', c and c' keeping the radius of the cylinder fixed ($a = 1$). Here, we use the terminology "a pair of opposite rotlets" to refer to two rotlets of equal strengths but of different sign. We also use the terminology "a pair of equal rotlets" to refer to two rotlets of same strengths and of same sign. These terminologies are also used for sources and stokeslets in subsequent subsections. Below we discuss the flow patterns due to rotlet(s) in the presence of a cylinder.

Figs. 3-4 show some flow patterns for an increasing sequence of values of the flow parameter λ_1 when a single rotlet is kept fixed at ($c = 2.5, \theta = 0$). For small values of the parameter $\lambda_1 \leq 0.5$, the flow patterns (Fig. 3(a)–(b)) do not change qualitatively. In fact, similar patterns have been noticed before when $\lambda_1 = 0$ (no-slip case) in [11]. Distinct qualitative changes occur in the flow patterns for values of $\lambda_1 > 0.5$. A nearly circular eddy first appears to the farther right of the rotlet which gradually moves closer to the rotlet as the value of λ_1 slowly increases to 0.75 (see Fig. 3(c)–Fig. 4(b)) During this process, the shape of the eddy also changes as it shrinks in overall size. In addition, the fluid exhibits a circulatory motion enclosing the cylinder, the rotlet, and the eddy. Further increases of λ_1 show interesting qualitative changes in the flow pattern. When $\lambda_1 = 0.77$, the single eddy disappears (or if it does not, it is very small and does not show up in this plot), but the circulatory motion prevails as shown in Fig. 4(c). Upon increasing the value of the slip parameter further, a different set of eddies appear around the cylinder (Fig. 4(d)). It is interesting to note that the presence of eddies for large values of the slip parameter ($\lambda_1 > 0.5$). This phenomenon is quite different from the flow pattern observed by Dorrepaal et. al. [11] in the case of no-slip.

In Figs. 5-6, flow patterns induced by a pair of equal rotlets past a cylinder are displayed for several values of the slip parameter. The rotlet on the right is located closer ($c = 2$) than the one on the left ($c' = 3$) to the cylinder. In this case, circulatory flow enclosing the cylinder and rotlets appears for $0 < \lambda_1 < 0.6$ (Fig. 5(a)-(b)). For $\lambda_1 > 0.6$ (see Fig. 5(c)-(d) and Fig. 6(a)-(d)), flow patterns change considerably. An eddy first appears to the right (farther away from the cylinder) of the rotlet which is closer to the cylinder. The flow topology in the vicinity of the rotlet to the left at (c', π) is qualitatively similar in these figures.

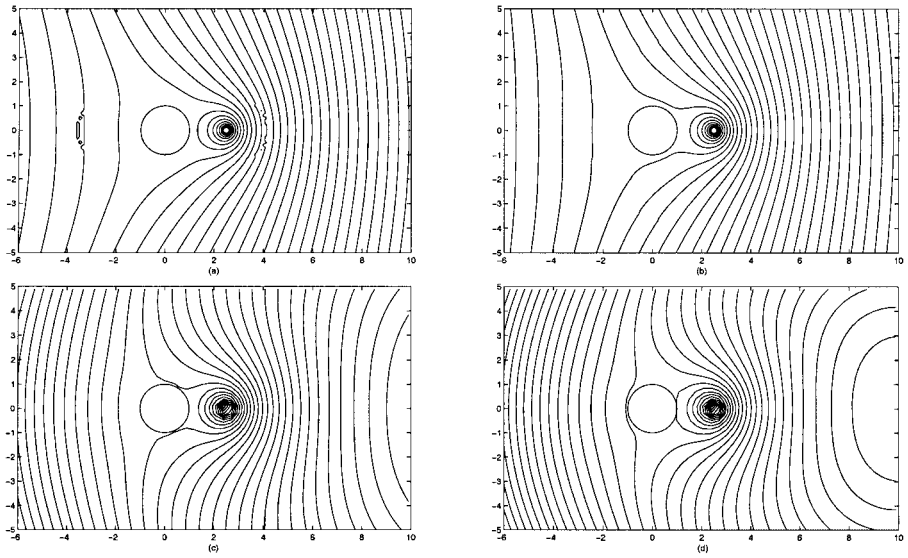

Figure 3. Flow past a cylinder in the presence of a single rotlet located at $(c = 2.5, 0)$ for different values of λ_1 . Here $F = 1$. (a) $\lambda_1 = 0.3$; (b) $\lambda_1 = 0.5$; (c) $\lambda_1 = 0.66$; (d) $\lambda_1 = 0.68$.

For higher values of of $\lambda_1 > 0.7$ (approximately) (see Fig. 6(a)-(d)), circulatory flow enclosing the cylinder and the rotlets appear.

Fig. 7 shows the streamline patterns for a pair of rotlets with (i) opposite strengths i.e., $F' = -F$ (Fig. 7(a)-(b)); and (ii) different strengths ($F' = 2F$ Fig. 7(c)-(f)). In case (i), for different locations of the rotlets, the flow is almost uniform in the far-field for smaller values of λ_1 . But for λ_1 close to 1, flow patterns are quite different near and far from the cylinder (see Fig. 7(b)). This shows that λ_1 alters the far-field behavior for various rotlet locations. In the case of a pair of rotlets with different strengths (case (ii)), more interesting eddy patterns appear in the flow field. Eddies enclosing the cylinder and rotlets are found to exist when $\lambda_1 = 0.2$ (Fig. 7(c)). When $\lambda_1 = 0.6$, a symmetric pair of eddies of nearly semi-circular shape appears right above and below the cylinder, in addition to the circulatory flow around the cylinder and the rotlets (see Fig. 7(d)). These eddies disappear for values of $\lambda_1 = 0.8, 0.9$ (see Fig. 7(e)-(f)). In fact, for these values of the slip parameter, an eddy of unusual size and shape enclosing the cylinder occurs (Fig. 7(e)). This latter eddy changes its shape if λ_1 is increased further (Fig. 7(f)). It should be pointed out that the location of the rotlets are fixed in the plots shown in Fig. 7(c)-(f). The change of locations also affect the generation of eddies and their structures which have not been shown here.

The velocity components with a rotlet at $(c, 0)$ in the presence of a cylinder

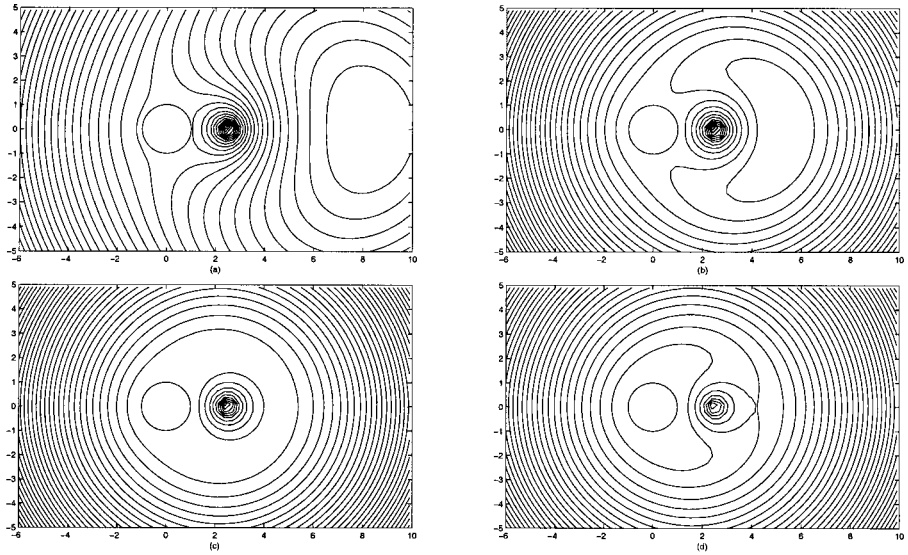

Figure 4. (continuation) Flow past a cylinder in the presence of a single rotlet located at $(c = 2.5, 0)$ for different values of λ_1. Here $F = 1$. (a) $\lambda_1 = 0.7$; (b) $\lambda_1 = 0.75$; (c) $\lambda_1 = 0.77$; (d) $\lambda_1 = 0.79$.

in closed form are given by

$$q_r = -F\sin\theta\left[\frac{c}{R_1^2} - \frac{a^2}{cR_2^2} - 2c\frac{1-\lambda_1}{\lambda_1}(a^2-r^2)\frac{r^{\frac{1-2\lambda_1}{\lambda_1}}}{a^{\frac{2}{\lambda_1}}}\int_0^{a^2/r}\rho^{\frac{1}{\lambda_1}}\frac{(\rho-\cos\theta)}{R_{1\rho}^2}d\rho\right], \tag{4.1.11}$$

$$q_\theta = F\left[\frac{r-c\cos\theta}{R_1^2} - -\frac{r-\frac{a^2}{c}\cos\theta}{R_2^2} + \frac{1-\lambda_1}{\lambda_1}\left(-2rI_1 + (a^2-r^2)\frac{\partial I_1}{\partial r}\right)\right], \tag{4.1.12}$$

The plots of q_θ versus θ on the upper half of the cylinder surface are shown in Fig. 8(a) for different values of λ_1. The location of the initial rotlet is fixed at $c = 2.0$. The plots show that with increasing θ, the fluid velocity on the upper half of the cylinder surface is first counter-clockwise, then clockwise and again back to counter-clockwise. Therefore, two stagnation points occur on the upper half of the surface for each value of λ_1 as can be seen in these figures since all the curves intersect the $q_\theta = 0$ line twice in this interval for θ. Fig. 8(b) shows the plots of the q_θ on the surface versus θ for a fixed value of $\lambda_1 = 0.5$ and for different rotlet locations. In this case, the plots are qualitatively also similar. The

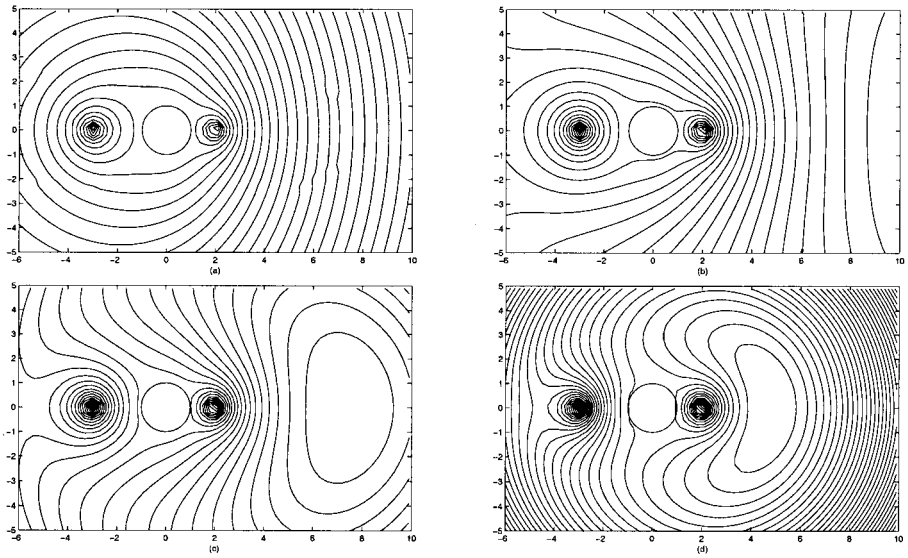

Figure 5. Flow past a cylinder in the presence of a pair of equal rotlets ($F = F' = 1$) located at $(c = 2, 0)$ and $(c' = 3, \pi)$ for various values of λ_1 . (a) $\lambda_1 = 0.2$;(b) $\lambda_1 = 0.6$; (c) $\lambda_1 = 0.65$; (d) $\lambda_1 = 0.7$.

two stagnation points on the upper surface of the cylinder for each value of c is also evident from this figure.

4.2. A circular cylinder and a potential source

The stream function for a potential source of strength S located at $r = c > a$, $\theta = 0$, in an unbounded fluid is

$$\psi_0 = S \tan^{-1}\left(\frac{r \sin\theta}{c - r\cos\theta}\right),$$

which has the Fourier expansion

$$\psi_0 = S \sum_{n=1}^{\infty} \frac{r^n}{nc^n} \sin n\theta. \tag{4.2.1}$$

From (3.1) and (4.2.1) we obtain

$$\alpha_n = \frac{S}{nc^n}, \quad \beta_n = \gamma_n = 0 \quad \delta_n = 1 \quad \text{for all} \quad n \geq 1.$$

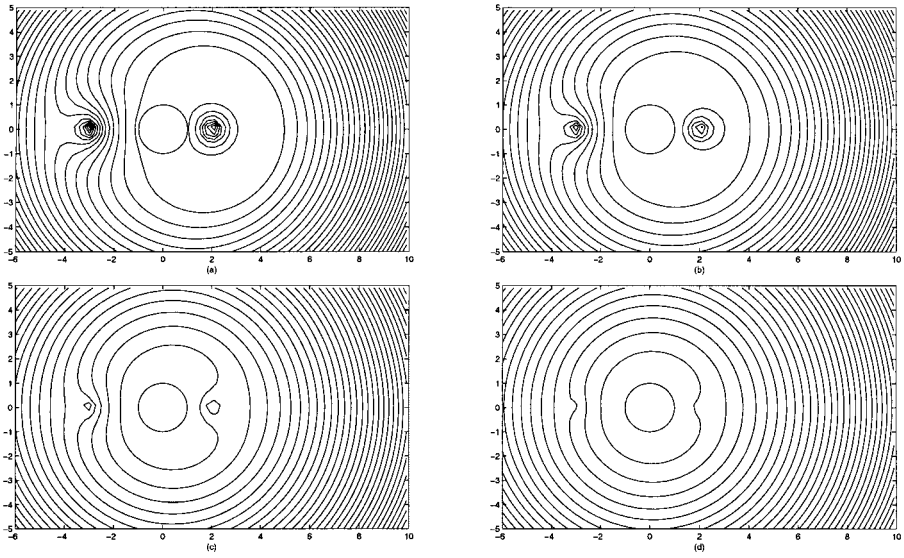

Figure 6. (continuation) Flow past a cylinder in the presence of a pair of equal rotlets ($F = F' = 1$) located at $(c = 2, 0)$ and $(c' = 3, \pi)$ for various values of λ_1 . (a) $\lambda_1 = 0.73$; (b) $\lambda_1 = 0.75$; (c) $\lambda_1 = 0.8$; (d) $\lambda_1 = 0.9$.

The scattering coefficients for a source-cylinder combination, calculated from (3.3) and (3.4), are

$$A_n = S\left(-1 + \frac{n}{n\lambda_1 + 1 - \lambda_1}\right)\frac{a^{2n}}{nc^n}\alpha_n, \tag{4.2.2}$$

$$B_n = -S\left(\frac{1}{n\lambda_1 + 1 - \lambda_1}\right)\frac{a^{2n-2}}{c^n}\alpha_n. \tag{4.2.3}$$

Substitution of (4.2.1)-(4.2.3) in (3.2) yields the Fourier series expansion for the stream function for a source-cylinder combination. The Fourier series can be summed to obtain the solution in a closed form. The exact expression for ψ in a source flow in the presence of a cylinder is

$$\psi(r,\theta) = S\left\{\tan^{-1}\left(\frac{r\sin\theta}{c - r\cos\theta}\right) - \tan^{-1}\left(\frac{a^2\sin\theta}{rc - a^2\cos\theta}\right) + \frac{1-\lambda_1}{\lambda_1}(a^2 - r^2)I_2\right\}, \tag{4.2.4}$$

where,

$$I_2 = \frac{r^{\frac{1-\lambda_1}{\lambda_1}}}{a^{\frac{2}{\lambda_1}}}\int_0^{a^2/r} \rho^{\frac{1}{\lambda_1}-2}\left[-\tan^{-1}\left(\frac{\rho\sin\theta}{c - \rho\cos\theta}\right) + \frac{\rho c\sin\theta}{R_{1\rho}^2}\right]d\rho, \tag{4.2.5}$$

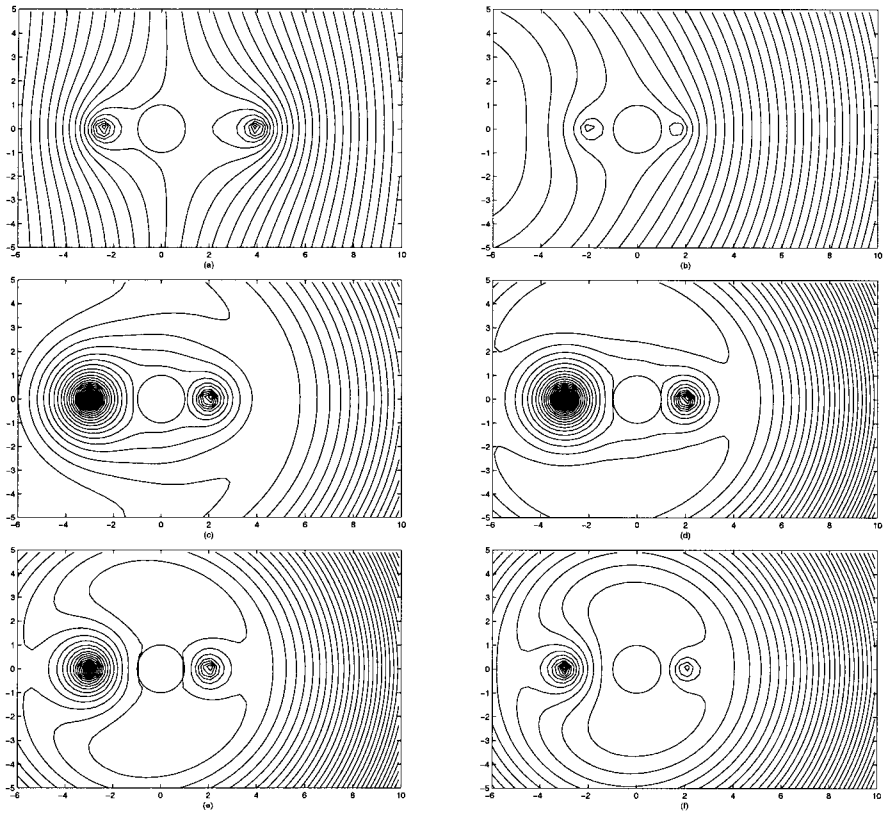

Figure 7. Flow past a cylinder in the presence of a pair of rotlets. (i) Opposite rotlets $(F = -F' = 1)$: (a) $\lambda_1 = 0.1$, $c = 4, c' = 2.5$; (b) $\lambda_1 = 0.7, c = 1.7, c' = 2$; (ii) Rotlets with different strengths $(F' = 2F = 2), c = 2.0, c' = 3$: (c) $\lambda_1 = 0.2$; (d) $\lambda_1 = 0.6$; (e) $\lambda_1 = 0.8$; (f) $\lambda_1 = 0.9$.

and $R_2, R_{1\rho}$ are as defined in (4.1.7). The solution for the no-slip case [13, 12] may be recovered from (4.2.4) by simply setting $\lambda_1 = 0$. The other limiting case occurs when $\lambda_1 = 1$ which corresponds to perfect-slip conditions. In this case, equation (4.2.4) reduces to

$$\psi(r,\theta) = S\left[\tan^{-1}\left(\frac{r\sin\theta}{c - r\cos\theta}\right) - \frac{r^2}{a^2}\tan^{-1}\left(\frac{a^2\sin\theta}{rc - a^2\cos\theta}\right)\right]. \qquad (4.2.6)$$

The solution for a source of strength S' located at (c', π) in the presence of a cylinder is

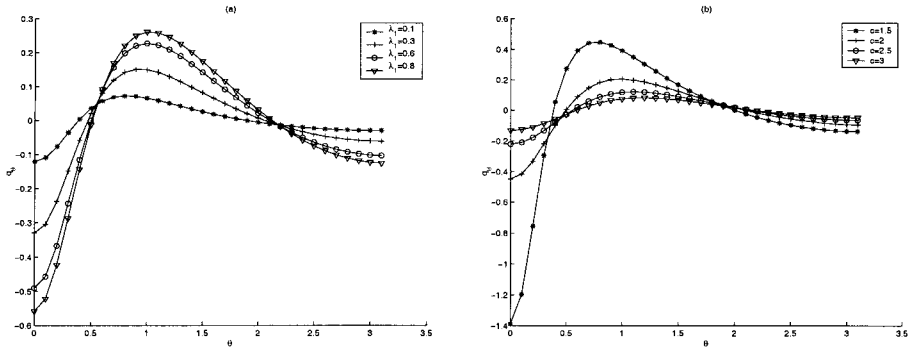

Figure 8. Fluid velocity on the surface of a cylinder of radius $a = 1$ due to a rotlet located at $(c, 0), c > 1$. (a) Effect of slip with fixed $c = 2.0$; (b) Effect of different rotlet locations for a fixed $\lambda_1 = 0.5$

$$\psi(r,\theta) = S'\left\{ \tan^{-1}\left(\frac{r\sin\theta}{c' + r\cos\theta}\right) - \tan^{-1}\left(\frac{a^2\sin\theta}{rc' + a^2\cos\theta}\right) + \frac{1-\lambda_1}{\lambda_1}(a^2 - r^2)I_2' \right\}, \tag{4.2.7}$$

where,

$$I_2' = \frac{r^{\frac{1-\lambda_1}{\lambda_1}}}{a^{\frac{2}{\lambda_1}}} \int_0^{a^2/r} \rho^{\frac{1}{\lambda_1}-2} \left[-\tan^{-1}\left(\frac{\rho\sin\theta}{c' + \rho\cos\theta}\right) + \frac{\rho c'\sin\theta}{R'^2_{1\rho}} \right] d\rho, \tag{4.2.8}$$

and $R'_{1\rho}$ is as defined in (4.1.12).

In Fig. 9, the flows induced by (i) a single source and (ii) a combination of source and sink in the presence of a cylinder are shown for various values of λ_1 . In case (i), expected flow patterns emerge and these do not change qualitatively for different values of the slip parameter (see Fig. 9(a)-(b)). In case (ii), the source is located to the right of the cylinder at $(c, 0)$, and the sink is to the left of the cylinder at (c', π) . Two typical scenarios are shown in Fig. 9(c)-(d). The location of the sink (to the left of the cylinder) is fixed in both of these plots. In Fig. 9(c), the sink is closer than the source to the cylinder ($c = 3.5, c' = 2.5$) whereas in Fig. 9(d), the source is closer than the sink to the cylinder ($c = 2, c' = 2.5$). It is rather striking that there is no direct transfer of fluid from the source to the sink in the finite plane. This is because the cylinder acts as a blocking mechanism for the flow in the Stokes regime. It may be seen from the representative plots Fig.9(c)-(d) that all the fluid expelled from the source goes away to infinity and all that drawn into the sink comes from infinity. Similar features were noticed in the case of source-sink flow in the presence of a cylinder with stick (no-slip) boundary conditions [12]. We have also plotted (not shown here) the flow patterns for

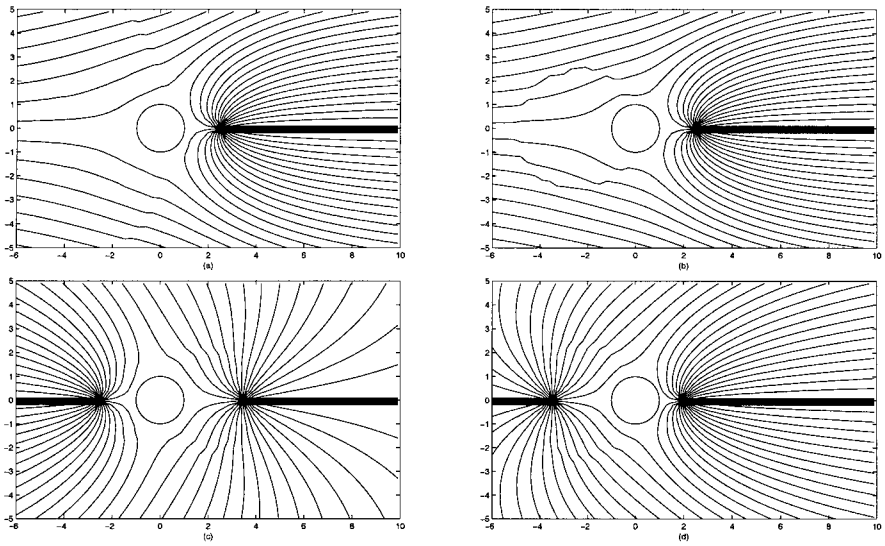

Figure 9. Flow past a cylinder in the presence of (i) a single source; and (ii) a source and sink; for various values of λ_1 . (i) single source $c = 2.5, S = 1$: (a) $\lambda_1 = 0.2$; (b) $\lambda_1 = 0.4$; (ii) Source and sink, $S = -S' = 1$: (c) $\lambda_1 = 0.6$, $c = 3.5, c' = 2.5$; (d) $\lambda_1 = 0.7$, $c = 2.0, c' = 3.5$.

various other values of λ_1, c and c' . Eddies do not appear in any of these cases as expected and the flow topologies are qualitatively similar to the cases discussed above.

The velocity components for a source at $(c, 0)$ in the presence of a cylinder are given by

$$q_r = -S\Bigg\{\frac{r(c\cos\theta - r)}{R_1^2} - \frac{a^2(rc\cos\theta - a^2)}{c^2R_2^2} + \frac{1-\lambda_1}{\lambda_1}(a^2 - r^2)\times \frac{r^{\frac{1-2\lambda_1}{\lambda_1}}}{a^{\frac{2}{\lambda_1}}}\int_0^{a^2/r}\rho^{\frac{1}{\lambda_1}}\left[\frac{1}{R_{1\rho}^2} - \frac{2c^2\sin^2\theta}{R_{1\rho}^4}\right]d\rho\Bigg\}, \tag{4.2.9}$$

$$q_\theta = S\Bigg\{\frac{c\sin\theta}{R_1^2} - \frac{a^2\sin\theta}{cR_2^2} + \frac{1-\lambda_1}{\lambda_1}\left(-2rI_2 + (a^2 - r^2)\frac{\partial I_2}{\partial r}\right)\Bigg\}. \tag{4.2.10}$$

In Fig. 10(a), fluid velocity on the surface is plotted against θ , $0 \le \theta \le \pi$, for several values of the slip parameter with location of the source kept fixed at $c = 2.0, \theta = 0.0$. As expected, flow on the surface is unidirectional between two

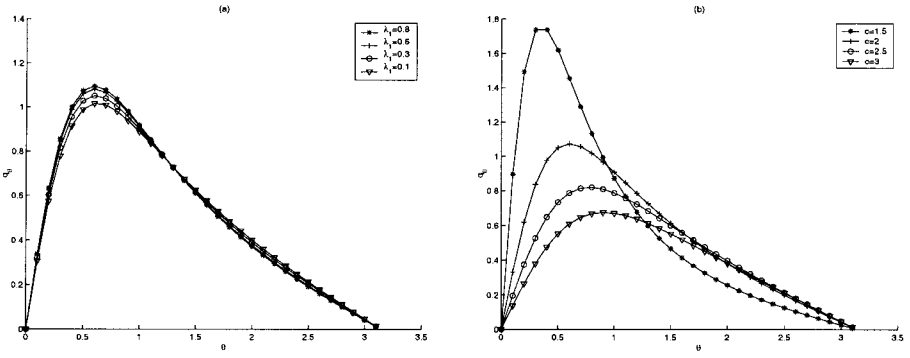

Figure 10. Fluid velocity on the surface of a cylinder of radius $a = 1$ due to a source located at $(c, 0), c > 1$. (a) Effect of slip with fixed $c = 2.0$; (b) Effect of different source locations for a fixed $\lambda_1 = 0.5$.

stagnation points $\theta = 0, \theta = \pi$, and the velocity on the surface attains a maximum somewhere in between whose value and location on the cylinder surface depend weakly on the value of λ_1. In fact, these plots show that the fluid velocity on little more than half of the cylinder surface changes little with λ_1. We also see in Fig. 9(a)-(b) that the slip parameter has little effect on the qualitative features of the flow fields in the Stokes regime which is consistent with our above observation. However, similar plots in Fig. 10(b) for several choices of source location with λ_1 now fixed at 0.5 show that surface velocity changes appreciably with changes in the location of the source. It also shows that with increasing c, maximum value of q_θ decreases and its location moves farther away from the stagnation point at $\theta = 0$.

4.3. A line stokeslet outside a circular cylinder

(i) Stokeslet with its axis along x-direction

We now consider a stokeslet of strength F_1 located at $r = c > a$, $\theta = 0$, whose axis is parallel to the positive x-direction. The stream function for a two-dimensional stokeslet in an unbounded fluid is given by

$$\psi_0 = F_1 r \sin\theta \log R_1,$$

with R_1 denoting the distance from the stokeslet. The Fourier expansion and the scattering coefficients in the present problem can be found in a manner similar to that explained for a rotlet/source problem. For the sake of brevity, we omit the details and give the exact expression for a stokeslet-cylinder combination. The

solution for the stream function is

$$\psi(r,\theta) = F_1 \sin\theta \left[r\log R_1 - r\log\left(\frac{c}{a}R_2\right) + \frac{1-\lambda_1}{\lambda_1}\left(\frac{r^2}{a^2}-1\right) I_3 \right], \qquad (4.3.1)$$

where

$$I_3 = \left(\frac{a^2}{r}\right)^{\frac{\lambda_1-1}{\lambda_1}} \int_0^{a^2/r} \rho^{\frac{1-\lambda_1}{\lambda_1}} \left(-\frac{\rho(\rho - c\cos\theta)}{R_{1\rho}^2} + \frac{(\rho^2-a^2)}{2R_{1\rho}^2} \right) d\rho. \qquad (4.3.2)$$

The relations R_2 and $R_{1\rho}$ are as defined in (4.1.7). The solutions for a rigid cylinder with stick $(\lambda_1 \to 0)$ or pure slip $(\lambda_1 \to 1)$ boundary conditions can be readily deduced from (4.3.1).

In a similar manner, the solution for a stokeslet of strength F_1' located at (c', π) may be derived. The expression for stream function in this case is given by

$$\psi(r,\theta) = F_1' \sin\theta \left[r\log R_1' - r\log\left(\frac{c'}{a}R_2'\right) + \frac{1-\lambda_1}{\lambda-1}\left(\frac{r^2}{a^2}-1\right) I_3' \right], \qquad (4.3.3)$$

where

$$I_3' = \left(\frac{a^2}{r}\right)^{\frac{\lambda_1-1}{\lambda_1}} \int_0^{a^2/r} \rho^{\frac{1-\lambda_1}{\lambda_1}} \left(-\frac{\rho(\rho + c'\cos\theta)}{R_{1\rho}'^2} + \frac{(\rho^2-a^2)}{2R_{1\rho}'^2} \right) d\rho. \qquad (4.3.4)$$

The relations R_1' and $R_{1\rho}'$ are as defined in (4.1.12).

The flow patterns due to a single stokeslet (with its axis along x-direction) in the presence of cylinder change little with λ_1 as shown in two typical cases ($\lambda_1 = 0.1$ and $\lambda_1 = 0.9$, see Fig. 11(a)-(b)). The far-field patterns in these cases are similar to that in similar stokeslet induced flow with no-slip boundary conditions (see Dorrepaal et al. [11]). The flow topologies for a pair of opposite stokeslets (with equal strength but opposite sign) in the presence of a cylinder are shown in Fig. 11(c)-(d). The stokeslet locations (r, θ) are $(c, 0)$, and (c', π) respectively. In all these flows, we find that the flow patterns hardly change with λ_1. Therefore, we have shown only two typical flow patterns. Stokeslet to the right is closer than the one to left ($c = 2, c' = 3$) in Fig. 11(c) and the situation is exactly reversed in Fig. 11(d) ($c = 3, c' = 2$). We see that the flow patterns in these two figures are therefore also reversed as expected, and only one of these two patterns can be considered as prototypical of these flows. Here, a symmetric pair of toroidal eddies appears in the neighborhood of the stokeslet that is closer to the cylinder whose shape or size do not change with variation in slip parameter. However, the stokeslet locations seem to play a dominant role in generating the eddies which we do not discuss in detail here. It may be worthwhile to point out that the toroidal eddy patterns shown in Fig. 9 are similar to the viscous eddies near planar boundaries [23, 24].

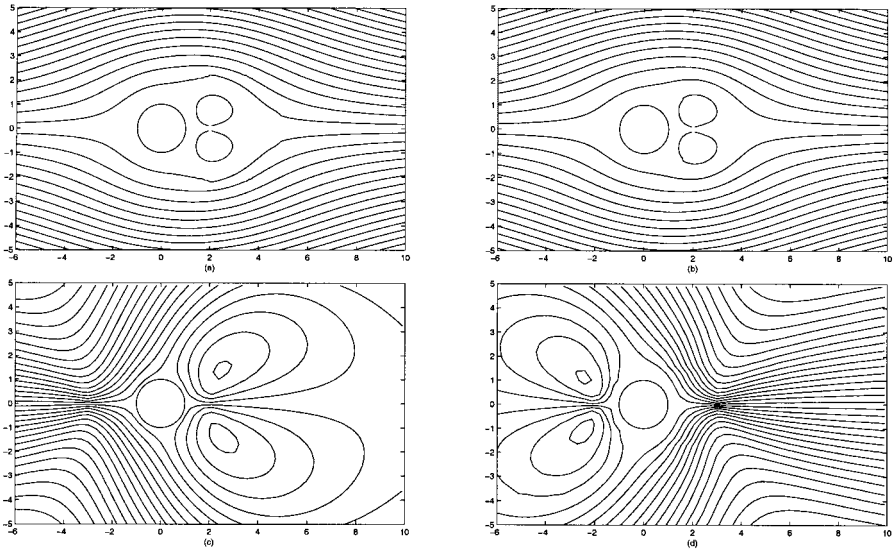

Figure 11. Flow past a cylinder in the presence of (i) a single stokeslet ($F_1 = 1$) and (ii) a pair of opposite stokeslets ($F_1 = -F_1' = 1$) for various values of λ_1 . The axis (axes) of the stokeslet(s) in both cases are taken to be along $x-$ direction. (a) $\lambda_1 = 0.1$; (b) $\lambda_1 = 0.9$; (c) $\lambda_1 = 0.8$; (d) $\lambda_1 = 0.2$.

The velocity components for a stokeslet-cylinder (with the stokeslet at $(c, 0)$ and its axis in the x-direction) combination are

$$q_r = -F_1 \cos\theta \left[\log R_1 - \log \frac{c}{a} R_2 + \frac{(1-\lambda_1)}{\lambda_1 r} \left(\frac{r^2}{a^2} - 1 \right) I_3 \right]$$
$$+ F_1 \sin\theta \left[\frac{rc \sin\theta}{R_1^2} - \frac{a^2 r \sin\theta}{cR_2^2} + \frac{(1-\lambda_1)}{\lambda_1 r} \left(\frac{r^2}{a^2} - 1 \right) \left(\frac{a^2}{r} \right)^{\frac{\lambda_1 - 1}{\lambda_1}} \times \right.$$
$$\left. \int_0^{a^2/r} \rho^{\frac{1-\lambda_1}{\lambda_1}} \left(-\frac{\rho c \sin\theta}{R_{1\rho}^2} + \frac{2\rho^2 c \sin\theta(\rho - c\cos\theta)}{R_{1\rho}^4} - \frac{(\rho^2 - a^2)\rho c \sin\theta}{R_{1\rho}^4} \right) d\rho \right], \tag{4.3.5}$$

$$q_\theta = F_1 \sin\theta \left[\log R_1 + \frac{r(r - c\cos\theta)}{R_1^2} - \log \frac{cR_2}{a} - \frac{r(r - \frac{a^2}{c}\cos\theta)}{R_2^2} \right.$$
$$\left. + \frac{(1-\lambda_1)}{\lambda_1} \left[\frac{2r}{a^2} I_3 + \left(\frac{r^2}{a^2} - 1 \right) \frac{\partial I_3}{\partial r} \right) \right]. \tag{4.3.6}$$

The limiting cases for a rigid cylinder with stick boundary conditions and for a shear-free cylinder with perfect slip conditions may be deduced from (4.3.5)–

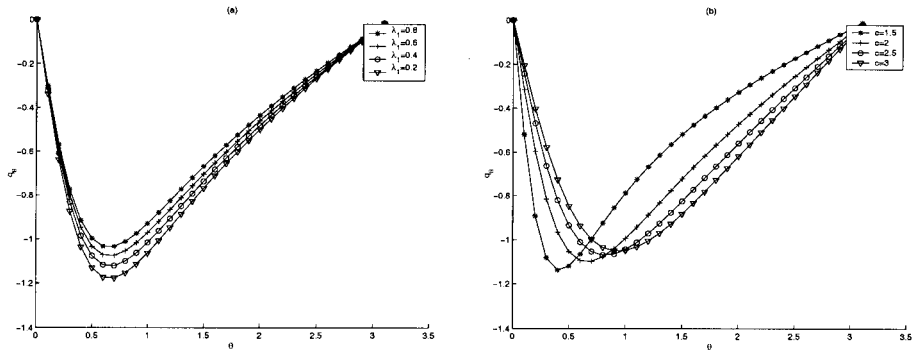

Figure 12. Fluid velocity on the surface of a cylinder of radius $a = 1$ due to a stokeslet with its axis along x-direction. (a) Effect of slip with fixed $c = 2.0$; (b) Effect of different stokeslet locations for a fixed $\lambda_1 = 0.5$.

(4.3.7). The plots of fluid velocity on the surface versus θ ($0 \leq \theta \leq \pi$) are shown in Fig. 12(a)-(b) for different λ_1 and c respectively. It shows that the flow clockwise on the cylinder and has stagnation points at obvious locations $\theta = 0, \pi$ for all choices of the slip parameter and stokeslet locations.

(ii) Stokeslet with its axis along y-direction

The stream function for a stokeslet, with axis along y-direction and strength F_2, located at $r = c > a, \theta = 0$ in an unbounded fluid motion is

$$\psi_0 = -F_2(r\cos\theta - c)\log R_1.$$

The function ψ_0 may be expanded in a similar manner explained in the rotlet problem and the scattering coefficients in the presence of a cylinder can be found from(3.1)–(3.4). The closed form stream function in the present case is

$$\psi(r,\theta) = \\ -F_2\left[(r\cos\theta - c)\log R_1 - \left(\frac{a^2}{c}\cos\theta - r\right)\log\left(\frac{cR_2}{a}\right) + \frac{1-\lambda_1}{\lambda_1}\left(\frac{r^2}{a^2} - 1\right)I_4\right], \tag{4.3.7}$$

where

$$I_4 = \left(\frac{a^2}{r}\right)^{\frac{\lambda_1-1}{\lambda_1}} \int_0^{a^2/r} \rho^{\frac{1-\lambda_1}{\lambda_1}} \left(\frac{(\rho\cos\theta - c)}{\rho} \log R_{1\rho} \right.$$
$$\left. - \cos\theta \log R_{1\rho} - \frac{(\rho\cos\theta - c)(\rho - c\cos\theta)}{R_{1\rho}^2} + \frac{(\rho^2 - a^2)}{2\rho} \frac{(\rho\cos\theta - c)}{R_{1\rho}^2} \right) d\rho. \tag{4.3.8}$$

It is clear that the distribution of singularities are involved in the image solution due to the slip-stick boundary conditions. In the limit $\lambda_1 \to 0$, (4.3.7) reduces to the solution obtained by Dorrepaal et al. [11] for a rigid cylinder and in the limit $\lambda_1 \to 1$, (4.3.7) yields the solution for a Stokeslet in the presence of a shear-free cylinder.

The solution for a stokeslet of strength F_2' located at (c', π) in the presence of a cylinder is

$$\psi(r,\theta) =$$
$$F_2' \left[(r\cos\theta + c') \log R_1' - \left(\frac{a^{2\,\prime}}{c} \cos\theta + r \right) \log\left(\frac{c' R_2'}{a} \right) + \frac{1-\lambda_1}{\lambda_1} \left(\frac{r^2}{a^2} - 1 \right) I_4' \right], \tag{4.3.9}$$

where

$$I_4' = \left(\frac{a^2}{r}\right)^{\frac{\lambda_1-1}{\lambda_1}} \int_0^{a^2/r} \rho^{\frac{1-\lambda_1}{\lambda_1}} \left(\frac{(\rho\cos\theta + c')}{\rho} \log {R'}_{1\rho} \right.$$
$$\left. - \cos\theta \log {R'}_{1\rho} - \frac{(\rho\cos\theta + c')(\rho + c'\cos\theta)}{{R'}_{1\rho}^2} + \frac{(\rho^2 - a^2)}{2\rho} \frac{(\rho\cos\theta + c')}{{R'}_{1\rho}^2} \right) d\rho. \tag{4.3.10}$$

Fig. 13 shows flow patterns due to a single stokeslet (with its axis along y-direction) in the presence of a cylinder for several values of λ_1. The flow topologies are seen to change significantly with λ_1. A circulatory flow surrounding the cylinder occurs for very small values of λ_1 (Fig. 13(a)). A substantial increase of the slip parameter generates other eddies in the flow field. Two sets of eddies, one enclosing the cylinder and the other in the neighborhood of the stokeslet, appear as shown in Fig. 13(b)-(c). The circulatory flow around the cylinder starts disappearing for slightly higher values of λ_1 (Fig. 13(d)). We also examined the flow pattern for values of of λ_1 close to 1 and the flow patterns are similar to the case shown in Fig. 13(a).

In Fig. 14, the flow fields in the case of a pair of opposite stokeslets are plotted for different values of λ_1. The flow pattern is shown in the range $0.5 \le \lambda_1 \le 0.78$.

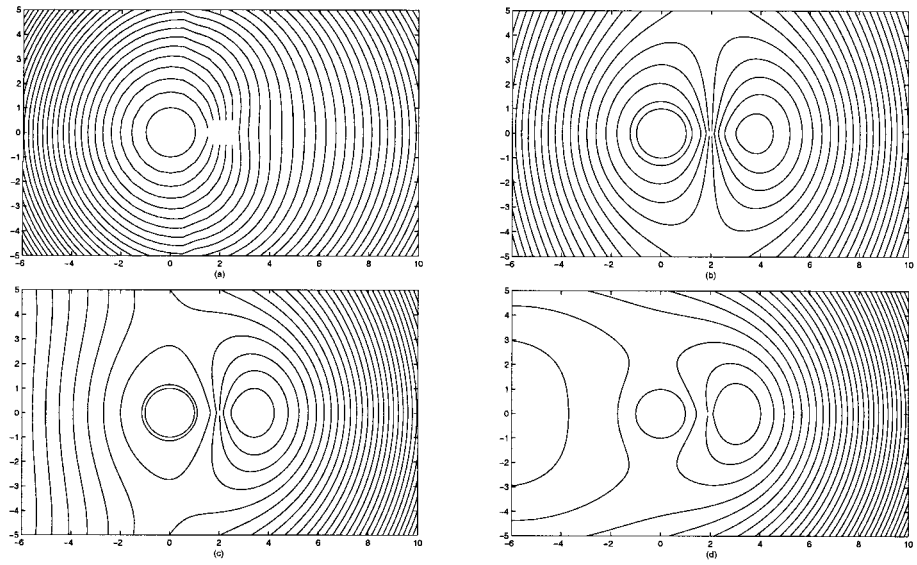

Figure 13. Flow past a cylinder in the presence of a Stokeslet with its axis along y-direction located at $(c = 2.0, 0)$ for different values of λ_1 ($F_2 = 1$). (a) $\lambda_1 = 0.1$; (b) $\lambda_1 = 0.35$; (c) $\lambda_1 = 0.37$; (d) $\lambda_1 = 0.4$;

When $\lambda_1 = 0.5$, two sets of closed streamlines occur: one in the neighborhood of the stokeslet at $(c, 0)$, another enclosing the stokeslet at (c', π) . In addition, a circulatory flow occurs enclosing the cylinder and the stokeslet at (c', π) (Fig. 14(a)). For $\lambda_1 > 0.5$, the fluid circulates around the cylinder and the stokeslet at $(c, 0)$ (Fig. 14(b)-(d)). It is evident from these plots that the shape of the eddies change with changes in the values of the slip parameter.

The flow patterns in the case of a pair of equal stokeslets are depicted in Figs. 15-16 for an increasing sequence of values of λ_1 . Circulatory flow as in Fig. 15(a)-(b) occurs for small values of the slip parameter ($\lambda_1 < 0.3$ (approximate value)) which subsequently disappears for higher values of λ_1 and more interesting flow patterns occur in the range $0.35 < \lambda_1 < 0.5$. Here three sets of eddies are generated enclosing the cylinder and stokeslets separately as evidenced from Fig. 15(c)-(d). The structure of these eddies change noticeably for various values of λ_1 in this range. For higher values of λ_1 , the rotational flow starts appearing again as seen from Fig. 16(a)-(d).

The velocity components for a stokeslet at $(c, 0)$ in the presence of a cylinder

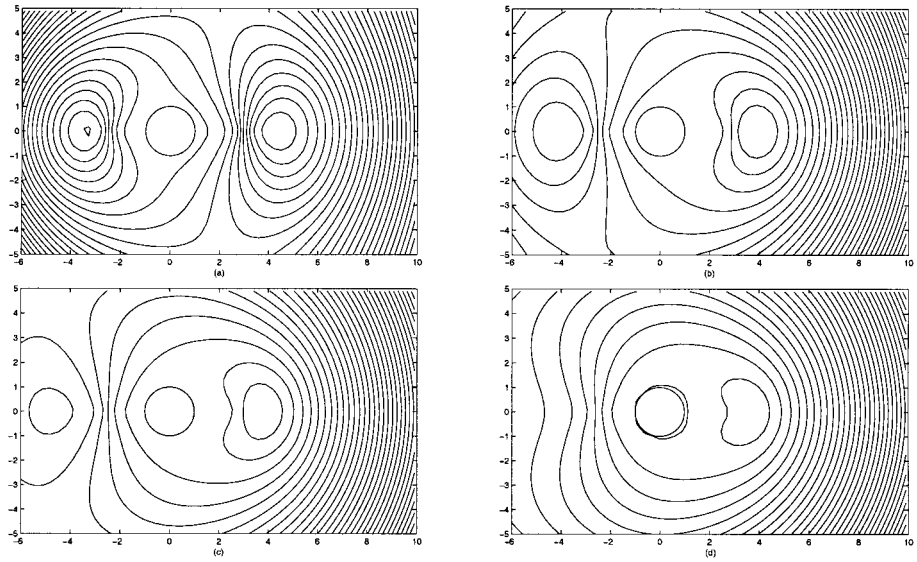

Figure 14. Flow past a cylinder in the presence of a pair of opposite stokeslets ($F_2 = -F_2' = 1$) with their axes along y-direction located at $(c = 3, 0), (c' = 2.5, \pi)$ for different values of λ_1 . (a) $\lambda_1 = 0.5$; (b) $\lambda_1 = 0.62$; (c) $\lambda_1 = 0.74$; (d) $\lambda_1 = 0.78$;

are

$$
\begin{aligned}
q_r = F_2 \Bigg\{ & \sin\theta \log R_1 + (r\cos\theta - c)\frac{c\sin\theta}{R_1^2} + \frac{a^2}{rc}\sin\theta \log\left(\frac{c}{a}R_2\right) \\
& - \frac{a^2}{c}\left(\frac{a^2}{c}\cos\theta - r\right)\frac{\sin\theta}{R_2^2} \quad + \frac{1-\lambda_1}{\lambda_1}\left(\frac{r^2}{a^2} - 1\right)\left[\frac{1}{\lambda_1 r}\left(\frac{a^2}{r}\right)^{\frac{\lambda_1 - 1}{\lambda_1}}\right. \\
& \int_0^{a^2/r} \rho^{\frac{1-\lambda_1}{\lambda_1}} \left((\rho\cos\theta - c)\frac{c\sin\theta}{R_{1\rho}^2} - \frac{rc\cos\theta\sin\theta}{R_{1\rho}^2} + \frac{\rho\sin\theta(\rho - c\cos\theta)}{R_{1\rho}^2} \right. \\
& - (\rho\cos\theta - c)\frac{c\sin\theta}{R_{1\rho}^2} + 2\frac{(\rho\cos\theta - c)(\rho - c\cos\theta)\rho c\sin\theta}{R_{1\rho}^4} \\
& \left.\left. + \frac{(\rho^2 - a^2)}{2\rho}\left(-\frac{\rho\sin\theta}{R_{1\rho}^2} + \frac{2(\rho\cos\theta - c)\rho c\sin\theta}{R_{1\rho}^4}\right)\right) d\rho \Bigg] \Bigg\}, \qquad (4.3.11)
\end{aligned}
$$

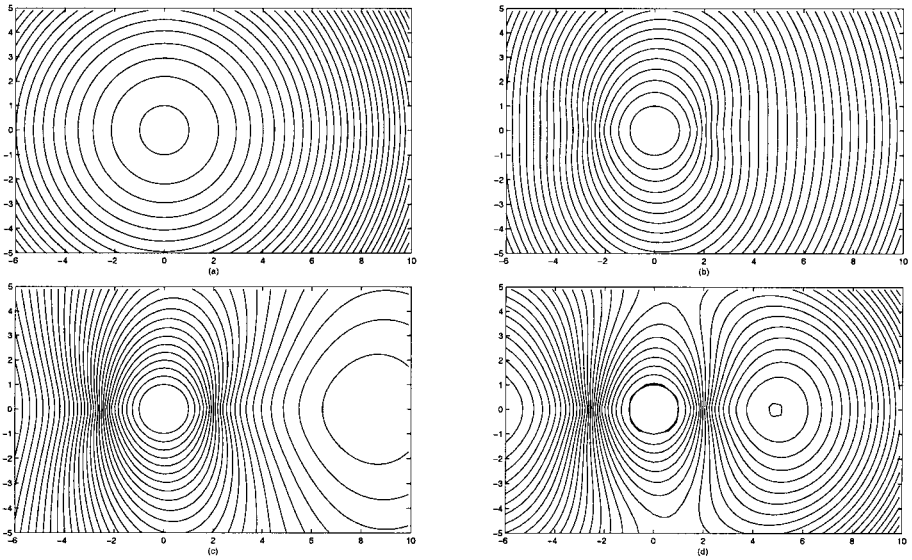

Figure 15. Flow past a cylinder in the presence of a pair of equal stokeslets ($F_2 = F_2' = 1$) with their axes along y-direction located at $(c = 2, 0), (c' = 2.5, \pi)$ for different values of λ_1 . (a) $\lambda_1 = 0.2$; (b) $\lambda_1 = 0.37$; (c) $\lambda_1 = 0.39$; (d) $\lambda_1 = 0.4$

$$q_\theta = -F_2\Bigg\{ \cos\theta \log R_1 + (r\cos\theta - c)\frac{(r - c\cos\theta)}{R_1^2} - \cos\theta \log \frac{c}{a} R_2$$
$$- (r\cos\theta - \frac{a^2}{c})\frac{(r - \frac{a^2}{c}\cos\theta)}{R_2^2} + \frac{1-\lambda_1}{\lambda_1}\left(\frac{2r}{a^2} I_4 + \left(\frac{r^2}{a^2} - 1\right)\frac{\partial I_4}{\partial r}\right)\Bigg\}. \quad (4.3.12)$$

Plots of fluid velocity on the surface of the cylinder against θ are shown in Fig. 17(a)-(b) for several values of λ_1 and c. They show that the location of the stagnation point at $\theta = \pi/2$ does not change with changes in the values of λ_1 (Fig. 17(a)), and change somewhat with c, the location of the stokeslet. We also not that the changes in fluid velocity on the surface is more dramatic with changes in λ_1 for a fixed c than with changes in c for a fixed λ_1.

5. Conclusion

Exact analytical solutions are presented for steady Stokes flows induced by singularities in the presence of a circular cylinder with stick-slip boundary conditions. The primary singularities considered here include (i) rotlet; (ii) potential source; (iii) stokeslet with its axis along x-direction and (iv) stokeslet with its axis along y-direction. The closed form solution given here in each case contains an integral

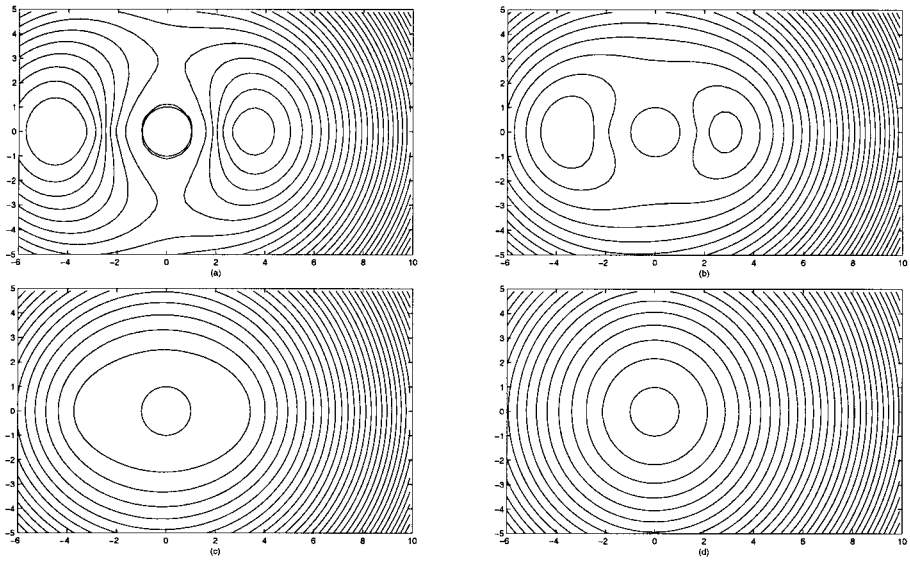

Figure 16. (continuation of Fig 15) Flow past a cylinder in the presence of a pair of equal stokeslets ($F_2 = F_2' = 1$) with their axes along y-direction located at $(c = 2, 0), (c' = 2.5, \pi)$ for different values of λ_1 . (a) $\lambda_1 = 0.46$; (b) $\lambda_1 = 0.48$; (c) $\lambda_1 = 0.53$; (d) $\lambda_1 = 0.6$.

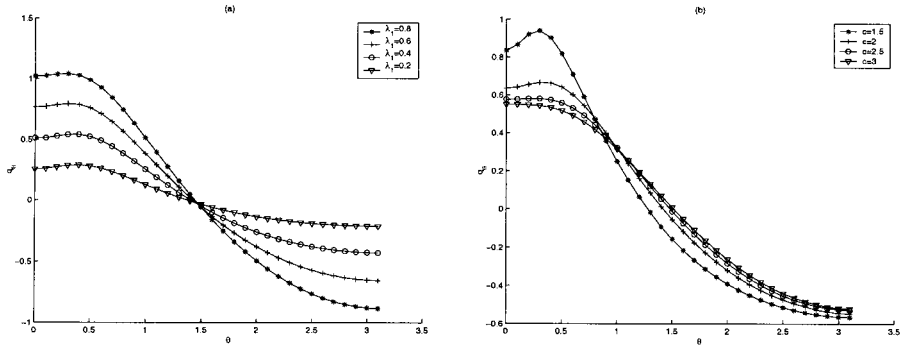

Figure 17. Fluid velocity on the surface of a cylinder of radius $a = 1$ due to a stokeslet with its axis along y-direction. (a) Effect of slip with fixed $c = 3.0$; (b) Effect of different stokeslet locations for a fixed $\lambda_1 = 0.5$.

involving the non-dimensional slip parameter λ_1. The flow fields change quite significantly with the slip parameter in most of the cases. In the case of flows induced by a single rotlet and a single stokeslet, eddy patterns emerge for several values of λ_1. The structure of these eddies most often changes with the slip parameter. The fluid velocity on the surface of the cylinder is plotted in each case. These plots show the extent to which the slip parameter and the primary singularity location may affect the fluid velocity and stagnation points on the surface. The flow fields produced by a pair of primary singularities in the presence of a cylinder are also discussed. Here again eddies of different size and shape are noticed for different values of λ_1. Finally, the solutions and flow patterns presented here clearly demonstrate the effect of slip on singularity driven flows.

6. Acknowledgment

This research has been partially supported by the interdisciplinary research program of the Office of the Vice President for Research and Associate Provost for Graduate Studies under grant IRI-98.

References

[1] G. G. Stokes, On the effect of internal friction of fluids on the motion of pendulums. *Trans. Camb. Phil. Soc.*, **9** (1851), 8-106 (see also *Scientific papers*, **3** (1901), 1-141, Cambridge University Press, Cambridge).

[2] H. Lamb, *Hydrodynamics*, 6th edition, Dover, New York (1932).

[3] J. Happel and H. Brenner, *Low Reynolds Number Hydrodynamics*. Martinus Nijhoff, The Hague, (1983).

[4] S. Kim and S. J. Karrila, *Microhydrodynamics: Principles and Selected Applications*, Butterworth, (1991).

[5] C. Pozrikidis, *Boundary Integral and Singularity Methods for Linearized Viscous Flow*, Cambridge University Press, (1992).

[6] C. Pozrikidis, *Introduction to Theoretical and Computational Fluid Dynamics*, Oxford University Press, (1996).

[7] S. Kaplun and P. A. Lagerstrom, Asymptotic expansion of Navier-Stokes solution for small Reynolds numbers. *J. Math. Mech.*, **6** (1957), 585-593.

[8] I. Proudman and J. R. A. Pearson, Expansions at small Reynolds numbers for the flow past a sphere and a circular cylinder. *J. Fluid Mech.*, **2** (1957), 237-262.

[9] C. W. Oseen, Über die Stokessche Formel und eine verwandte Aufgabe in der Hydrodynamik. *Ark. Mat. Astr. Fys.*, **6** (1910), 29.

[10] G. B. Jeffery, The rotation of two circular cylinders in a viscous fluid. *Proc. Roy. Soc. London, Ser. A*, **101** (1922), 169-174.

[11] J. M. Dorrepaal, M. E. O'Neill and K. B. Ranger, Two-dimensional Stokes flows with cylinders and line singularities. *Mathematika*, **31** (1984), 65-75.

[12] S. H. Smith, Some limitations of two-dimensional unbounded Stokes flow. *Phys. Fluids*, **A2** (1990), 1724-1730.

[13] A. Avudainayagam and B. Jothiram, No-slip images of certain line singularities in a circular cylinder. *Int. J. Engg. Sci.*, **25** (1987), 1193-1205.

[14] R. D. Present, *Kinetic Theory of Gases*, McGraw Hill, New York (1958).
[15] A. B. Basset, *A Treatise on Hydrodynamics*, Volume 2, Deighton, Bell and co., Cambridge, (1888).
[16] B. U. Felderhof, Force density on a sphere in linear hydrodynamics. I. Fixed sphere, stick boundary conditions. *Physica A*, **84** (1976a), 557-568.
[17] B. U. Felderhof, Force density on a sphere in linear hydrodynamics. II. Moving sphere, mixed boundary conditions. *Physica A*, **84** (1976b), 569-576.
[18] R. Schmitz and B. U. Felderhof, Creeping flow about a sphere. *Physica A*, **92** (1978), 423-437.
[19] B. U. Felderhof and R. B. Jones, Hydrodynamics scattering theory of flow about a sphere. *Physica A*, **136** (1986), 77-98.
[20] S. A. Wymer, A. Lakhtakia and R. S. Engel, Extinction cross-section of an arbitrary body in a viscous incompressible fluid. *Phys. Rev. E*, **52** (1995), 1857-1865.
[21] S. A. Wymer, A. Lakhtakia and R. S. Engel, The Huygens principle for flow around an arbitrary body in a viscous incompressible fluid. *Fluid Dynamics research*, **17** (1996), 212-223.
[22] H. Power, The completed double layer boundary integral equation method for two-dimensional stokes flow. *IMA J. Appl. Math.*, **51** (1993), 123-145.
[23] N. Liron and J. R. Blake, Existence of viscous eddies near boundaries. *J. Fluid Mech.*, **107** (1981), 109-129.
[24] J. R. Blake and S. R. Otto, Ciliary propulsion, chaotic filtration and a 'blinking stokeslet'. *J. Engg. Math.*, **30** (1996), 151-168.

D. Palaniappan and Prabir Daripa
Department of Mathematics
Texas A&M University
College Station, Texas-77843
USA
e-mail: prabir.daripa@math.tamu.edu

(Received: March 14, 2001; revised: August 9, 2001)